Available online at www.sciencedirect.com
ScienceDirect
International Journal of Heat and Mass Transfer 50 (2007) 4360–4370
International Journal of HEAT and MASS TRANSFER
www.elsevier.com/locate/ijhmt

Temperature wall modelling for large-eddy simulation in a heated turbulent plane channel flow

Y. Benarafa [a], O. Cioni [a], F. Ducros [a,*], P. Sagaut [b]

[a] Laboratoire de Modélisation et Développement Logiciels, DEN/DER/SSTH, CEA Grenoble, 17 Rue des Martyrs, 38054 Grenoble Cedex 9, France
[b] Laboratoire de Modélisation en Mécanique, Université Pierre et Marie Curie – Paris 6, 4, Place Jussieu, Case 162, 75252 Paris Cedex 05, France

Received 7 November 2005; received in revised form 10 August 2006
Available online 23 May 2007

Abstract

Industrial flows are often wall-bounded, characterized by a high Reynolds number turbulence and a strong unsteadiness. Large-eddy Simulations applied to this kind of flows require a heavy mesh resolution which is out of reach of the nowadays computational power. Wall models are usually used to alleviate this constraint. However, very few of them are dedicated to the temperature field. Besides, most of these wall models are based on equilibrium laws which are not able to take into account the unsteadiness of the flow in the near-wall region. In this study, an original thermal wall model, inspired from the TBLE wall model of Balaras et al. [E. Balaras, C. Benocci, U. Piomelli, Two-layer approximate boundary conditions for large-eddy simulations, AIAA J. 34 (6) (1996) 1111–1119], is developed and implemented in the CEA (French Atomic Center) Trio_U code and assessed on a heated and turbulent plane channel flow configuration. The investigated friction Reynolds numbers are 395, 1020 and 4800, and the Prandtl number is taken equal to 0.71.

Keywords: Trio_U; Large-eddy simulation; Wall models; TBLE; Temperature

1. Introduction

Industrial flows are often characterized by a high Reynolds number, and they are also often turbulent and wall-bounded flows. In the nuclear industry, for instance, unsteadiness of such flows is a key feature for safety studies. In particular, the near-wall unsteadiness of the flow is usually a crucial feature for conjugate heat transfer. Unsteady Reynolds Averaged Navier–Stokes approach (URANS) is commonly used in the industrial world and is only able to take into account low frequency features of the flow. Large-eddy simulation (LES) seems to be a relevant technique to perform flow simulations able to capture accurately the major part of the unsteadiness of the flow.

Wall-resolved LES requires a tremendous mesh refinement in the near-wall region for high Reynolds number flows and may imply the same computational cost as a Quasi Direct Numerical Simulation (QDNS). Many studies attempted to evaluate the LES mesh requirements for wall-bounded flows. Chapman [11] was probably the first to highlight the Reynolds number dependency of the mesh requirements in the near-wall region. He evaluated that the number of grid points should scale as $Re^{1.8}$ in the inner layer of the boundary layer, and as $Re^{0.4}$ in the outer layer. Piomelli and Balaras [25], using the same estimation tools, consider that in a boundary flow case, if the Reynolds number is about one million, 99% of the computational nodes should be used to compute the inner layer given that this latter represents only 10% of the boundary layer. Moreover, Baggett et al. [4] estimate that the required LES mesh for a plane channel flow scales as Re_τ^2. Re_τ is the friction Reynolds number based on the friction velocity u_τ, the half channel height h and the molecular viscosity ν. The friction Reynolds number can be related to the "classical" Reynolds number thanks to the Dean correlation [14]. According to this criterion and the Dean correlation,

* Corresponding author.
E-mail address: frederic.ducros@cea.fr (F. Ducros).

0017-9310/$ - see front matter © 2007 Elsevier Ltd. All rights reserved.
doi:10.1016/j.ijheatmasstransfer.2006.12.038

a flow with a Reynolds number of one hundred million requires approximately a mesh of 10^{12} nodes to be computed. With the available computing power, a simulation with a mesh of 10^9 nodes remains very rare (see Ref. [2], for instance). Following Spalart [28], considering that the computer power increases by a factor of 5 every 5 years, one can estimate that the QDNS will be out of reach until 2070. As a consequence, wall-resolved LES applied to wall-bounded flow configurations for high Reynolds numbers implies a prohibitive computational cost for the nowadays computer power.

In order to alleviate this mesh constraint, many research works have been performed to develop wall models (see [25] or [26] for an exhaustive review). These latters are built to approximate the wall boundary conditions, allowing the use of coarser meshes. Wall models for large-eddy simulation can be divided into two categories. The first one concerns the wall models based on equilibrium laws such as the logarithmic law. The other one consists of using a different approach (most of the time a RANS approach) in the near-wall region to provide the coarse grid LES with an accurate estimate of the wall shear stress.

The latter approach was pionneered by Balaras et al. [5]. Introducing a wall model referred to as two-layer model or thin boundary layer equations (TBLE), these authors embedded a one-dimensional grid between the wall and the first LES computation node. A RANS equation is solved on this inner mesh. As an upper boundary condition, the outer LES mesh supplies the inner mesh with the velocity and the pressure gradient computed at the first LES node. In return, the TBLE inner mesh using a no-slip condition at the wall provides the LES outer mesh with a wall shear stress. The key of this method is that the pressure gradient is assumed to be constant in the fine mesh (i.e. in the wall-normal direction), avoiding solving a Poisson equation inversion for incompressible flows, hence a huge reduction of the computational cost. Several variants of the TBLE wall model have been developed (see [7–9,15,31]), which will be discussed in Section 2.3. A second attempt of the same kind is the Detached Eddy Simulation (DES) used as a wall model by Nikitin et al. [24]. In this method, the inner layer is resolved thanks to a RANS approach. Schmidt et al. [27] also investigated a two-layer approach. Contrary to the two previous methods, the inner mesh is not resolved by a RANS model but by the one-dimensional turbulence (ODT) model introduced by Kerstein [20]. In this latter, the one-dimensional field is obtained by two mechanisms: the first one is the molecular diffusion which is solved in the one-dimensional grid and a sequence of instantaneous transformations, qualified as "eddy events", which are determined by a non-linear probabilistic model.

Despite the increase of these recent developments, wall models are only dedicated to the velocity field and none of them addresses the problem of the temperature field. A wall model for the temperature field should supply the LES with a normal heat flux. Thus, developing temperature wall models for high Reynolds number flows with thermal boundary condition as imposed temperature and conjugate heat transfer may appear as a relevant approach.

This study aims at investigating further the TBLE wall model and applying this approach to the temperature field to evaluate accurately the wall heat flux, the emphasis being put on the unsteadiness of the flow and the coarseness of the grid.

The numerical setup and the modelling framework will be presented in Section 2. Then the results obtained in a heated plane channel flow configuration will be discussed (Section 3). Finally, some conclusions and future work will be given (Section 4).

2. Numerical setup and modelling framework

2.1. Governing equations

In this study the flow is incompressible and turbulent so that the mass conservation, the momentum filtered equations and the temperature transport equation acting as a passive scalar can be expressed as follows:

$$\frac{\partial \bar{u}_j}{\partial x_j} = 0 \tag{1}$$

$$\frac{\partial \bar{u}_i}{\partial t} + \frac{\partial \bar{u}_i \bar{u}_j}{\partial x_j} = -\frac{1}{\rho}\frac{\partial \overline{P}}{\partial x_i} + 2\frac{\partial}{\partial x_j}\left((\nu + \nu_{\mathrm{sgs}})\overline{S}_{ij}\right) \tag{2}$$

$$\text{with} \quad \overline{S}_{ij} = \frac{1}{2}\left(\frac{\partial \bar{u}_i}{\partial x_j} + \frac{\partial \bar{u}_j}{\partial x_i}\right)$$

$$\frac{\partial \overline{T}}{\partial t} + \frac{\partial \bar{u}_j \overline{T}}{\partial x_j} = \frac{\partial}{\partial x_j}\left((\alpha + \alpha_{\mathrm{sgs}})\frac{\partial \overline{T}}{\partial x_j}\right) + Q_f \tag{3}$$

where $\overline{(.)}$ is LES filter operator. ν_{sgs} is a subgrid-scale viscosity. ν is the molecular viscosity and α is the thermal diffusivity. Q_f is a heat source term to create heat flux in the channel flow.

The selective structure function model (for more details about this subgrid-scale model see [22]) is used for LES computations. Given the Prandtl number used in this study ($Pr = 0.71$), the turbulent diffusivity α_t is determined assuming that the subgrid-scale Prandtl number ($Pr_{\mathrm{sgs}} = \frac{\nu_{\mathrm{sgs}}}{\alpha_{\mathrm{sgs}}}$) is constant and equal to 0.9 (see the work of Kawamura et al. [19] for the justification of this assumption).

The flow configuration considered is well-known (see for example [21] or [1]) and consists in a bi-periodic channel flow. The x-direction is the streamwise direction (see Fig. 1). To deal with pressure loss induced by the friction effects and to enforce a constant mass flow rate in the channel, a source term is added to the momentum equation at each time steps.

The correlation of Dean [14] is used to prescribe a friction Reynolds number Re_τ to the flow. It has to be noted that this correlation is only valid for a friction Reynolds number lying between 350 and 2×10^4.

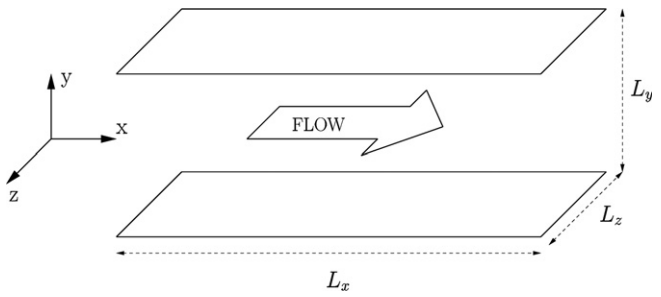

Fig. 1. Plane channel flow configuration.

2.2. Numerical procedure

All the computations presented in this study were performed with the TRIO_U code. This object oriented code solves Eqs. (1)–(3) using a mixed finite volume/finite element approach for both structured and unstructured grids (see the Ref. [10] for details about the implementation). For the present study, structured grids are considered; unknowns are located on a staggered mesh and the discrete form of the equations is solved using a matrix projection scheme which is a variant of the SOLA method originally developed by Hirt et al. [18] (more details about this projection method are given in the Ref. [16]).

The divergence free constraint is enforced using the projection method mentioned above: the Poisson's equation is solved using an iterative conjugate gradient method.

Time advancement is performed using a third-order Runge–Kutta explicit scheme. For the momentum equation (2), we use a centred second-order scheme for convection and diffusion terms. For the temperature transport equation (3), a centred second-order scheme and a QUICK scheme, as suggested by Châtelain et al. [12], have been respectively used for the diffusive and the convective terms.

2.3. Wall modelling

2.3.1. Wall models based on equilibrium laws

A wall model is designed to provide the wall gradient of a considered field (velocity or temperature) by modelling the physics of the turbulent wall flow rather than capturing it directly. The wall shear stress will be evaluated thanks to the friction velocity u_τ ($\tau_w = \rho u_\tau^2$, τ_w being the skin friction and ρ being the fluid density) instead of the following computation:

$$\tau_{xy}^w = \nu \frac{\partial u_x}{\partial y} \simeq \nu \frac{u_x^1 - u_x^w}{y_1 - y_w} \tag{4}$$

where u_x^1 is the streamwise velocity at the first velocity node, u_x^w is the flow velocity at the wall, $y_1 - y_w$ is the distance from the first velocity node to the wall, and τ_{xy}^w is the wall shear stress.

Most of common wall models are based on equilibrium laws such as the logarithmic law (see Grotzbach [17]):

$$U^+ = y^+; \quad \text{if } y^+ < 5 \quad \text{(Viscous sublayer)} \tag{5}$$

$$U^+ = \int_0^{y^+} \frac{2\,\mathrm{d}\alpha}{1 + \sqrt{1 + 4\,\mathrm{lm}_+^2(\alpha)}}; \quad \text{if } 5 < y^+ < 30 \tag{6}$$

$$\text{with} \quad \mathrm{lm}_+(\alpha) = \chi\alpha^+\left(1 - \exp\left(-\frac{\alpha}{26}\right)\right) \quad \text{(Buffer layer)}$$

$$U^+ = \frac{1}{\chi}\ln(y^+) + A \quad \text{if} \quad y^+ > 30 \quad \text{(Logarithmic layer)} \tag{7}$$

where $U^+ = \frac{U}{u_\tau}$ is the reduced velocity and y_w^+ is the wall distance in wall units. Then the wall shear stress is evaluated by the computation of friction velocity.

To model the wall normal heat flux ϕ_w on a coarse mesh, the Kader law is used. It is expressed as follows:

$$\frac{T - T_w}{T_\tau} = Pry^+ e^{-\Gamma} + [2.12\ln[(1 + y^+)C] + \beta]e^{-1/\Gamma} \tag{8}$$

with

$$\Gamma = \frac{10^{-2}(Pry^+)^4}{1 + 5Pr^3 y^+} \quad \text{and} \quad C = \frac{1.5(2 - y/h)}{1 + 2(1 - y/h)^2}$$

In this second formula, the temperature is normalized by the friction temperature T_τ which is defined as

$$T_\tau = \frac{\alpha}{u_\tau}\left(\frac{\partial T}{\partial y}\right)_w = \frac{\phi_w}{\rho C_p u_\tau} \tag{9}$$

Then, the friction temperature (and then the wall heat flux) is computed thanks to the Kader law (8) and provided to the LES computation.

2.3.2. Velocity and temperature TBLE wall model

The TBLE wall model has been developed for the first time by Balaras et al. [5]. As explained in the introduction, this wall model relies on the embedding of a one-dimensional mesh where RANS Thin Boundary Layer Equations are solved to supply the LES computation with the wall shear stress. In return, the LES first computation node will impose the upper boundary condition ensuring the continuity of the velocity or temperature field at the interface. Unlike the computation of Balaras et al., it was chosen in this study to embed the one-dimensional mesh at the center of the cell as it is shown in Fig. 2 instead of localizing it between the velocity nodes and the wall. Then, given that a staggered mesh was used in this study, the first node velocity of the LES mesh was interpolated at the center of the cell to provide the TBLE mesh with an upper boundary condition. On this mesh, the solved equations for the TBLE velocity field ($i = 1$ or 3) are the following:

$$\frac{\partial u_i}{\partial t} - \frac{\partial}{\partial y}\left((\nu + \nu_t)\frac{\partial u_i}{\partial y}\right) = -\frac{\partial P}{\partial x_i} - \frac{\partial(u_i u_j)}{\partial x_j} \tag{10}$$

Since the Poisson equation is not solved to enforce the mass conservation, the TBLE normal velocity is computed integrating the mass conservation equation:

$$v(y) = -\int_0^y \left(\frac{\partial u}{\partial x}(\alpha) + \frac{\partial w}{\partial z}(\alpha)\right)\mathrm{d}\alpha \tag{11}$$

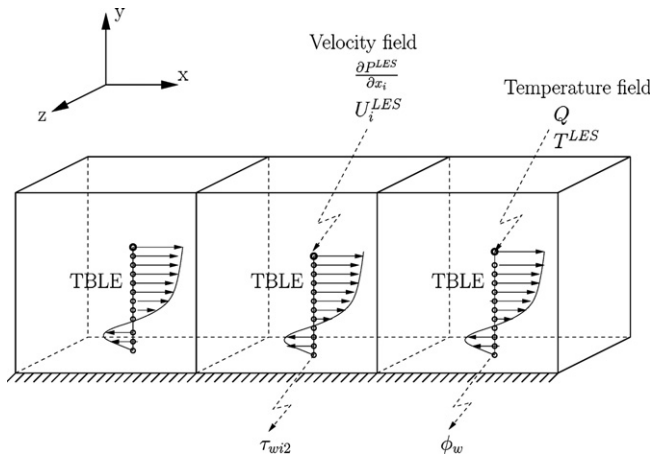

Fig. 2. Near-wall TBLE one-dimensional mesh and staggered LES mesh. As shown in this picture, the TBLE wall model can take into account an adverse pressure gradient. Obviously, this situation is not encountered in a plane channel flow.

The resulting normal velocity is used to compute the convection terms. The turbulent viscosity ν_t is evaluated thanks to a mixing length model with the Van Driest damping function:

$$\nu_t = D_{vd}(\kappa y)^2\left(\left(\frac{\partial u}{\partial y}\right)^2+\left(\frac{\partial w}{\partial y}\right)^2\right)^{1/2} \quad \text{with}$$

$$D_{vd} = 1-\exp\left[-\left(\frac{y^+}{25}\right)^3\right] \tag{12}$$

Various boundary conditions have been tested at the interface between the inner TBLE one-dimensional grid and the outer LES mesh. Balaras et al. [5] proposed to use the velocity provided by the first near-wall node of the LES mesh as a boundary conditions and the pressure gradient as a source term to the TBLE equations. In addition to these latters, Diurno et al. [15] attempted to impose the continuity of the shear stress or the one of the turbulent viscosity. They conclude that enforcing turbulent viscosity continuity is the best choice for numerical stability reasons. Wang and Moin [31], considering a trailing edge flow, did also connect the subgrid-scale viscosity to the TBLE turbulent viscosity at the interface between the LES outer mesh and the TBLE inner mesh.

In the present TBLE implementation, due to the staggered grid arrangement, the first LES node is interpolated at the center of the cell to compute the upper boundary conditions for the TBLE mesh.

On the inner TBLE mesh, the temperature field is also computed solving the following equation:

$$\frac{\partial T}{\partial t}-\frac{\partial}{\partial y}\left((\alpha+\alpha_t)\frac{\partial T}{\partial y}\right) = Q-\frac{\partial(Tu_j)}{\partial x_j} \tag{13}$$

As for the LES computation, the turbulent Prandtl number is considered constant ($Pr_t = 0.9$) so that the turbulent diffusivity α_t is proportional to the turbulent visco-

Table 1
Mesh parameters in wall units

Re_τ	Δx^+	Δy^+	Δz^+
395	78	25	39
1020	200	64	100
4800	943	300	472

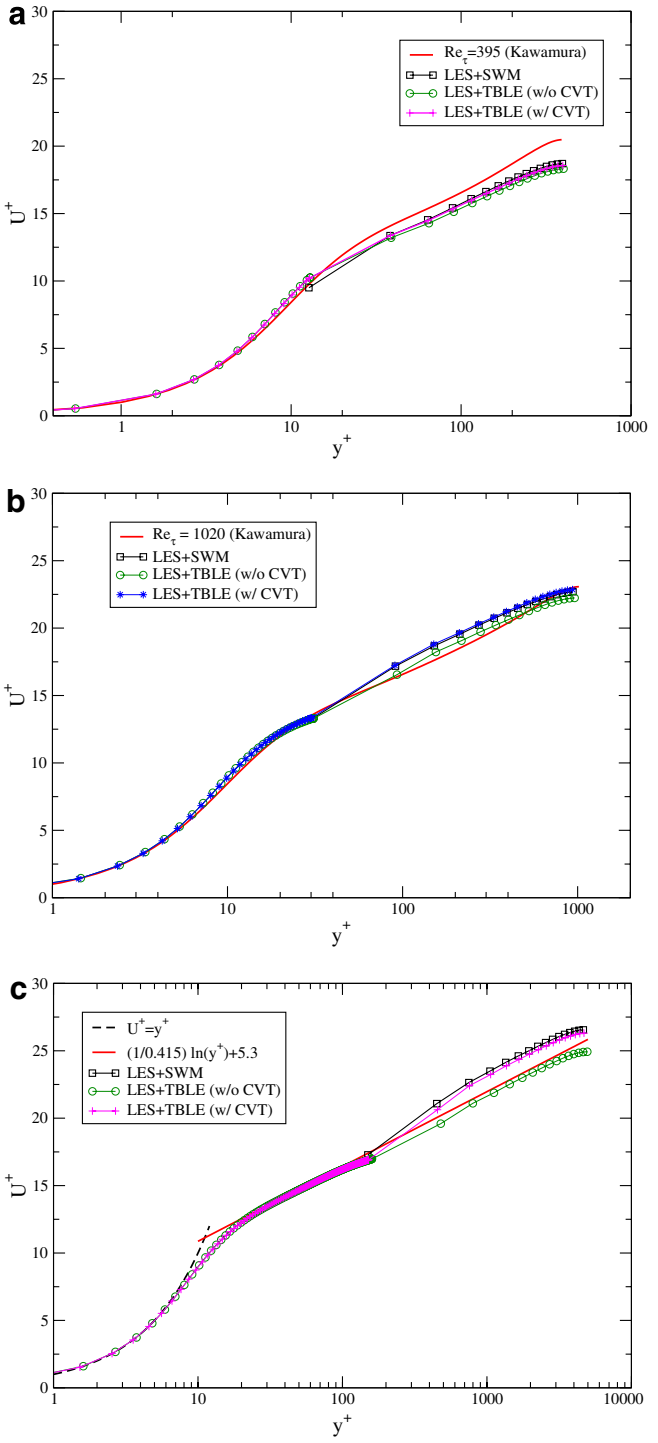

Fig. 3. Mean streamwise velocity profiles: (a) $Re_\tau = 395$, (b) $Re_\tau = 1020$ and (c) $Re_\tau = 4800$.

sity. As for the TBLE wall model for the velocity field, the thermal TBLE wall model requires the value of the temperature at the first temperature node (located at the center of the LES cell) and the source term Q. In return, the thermal TBLE wall model provide the LES outer mesh with a wall heat flux ϕ_w.

To preserve the unsteadiness information provided by the LES computation, a particular numerical procedure, based on an Unsteady RANS method, was used to solve Eqs. (10) and (13). This numerical procedure was presented and discussed in Ref. [6].

3. Results and discussion

To study the behavior of the TBLE model in various boundary layer configurations, three friction Reynolds

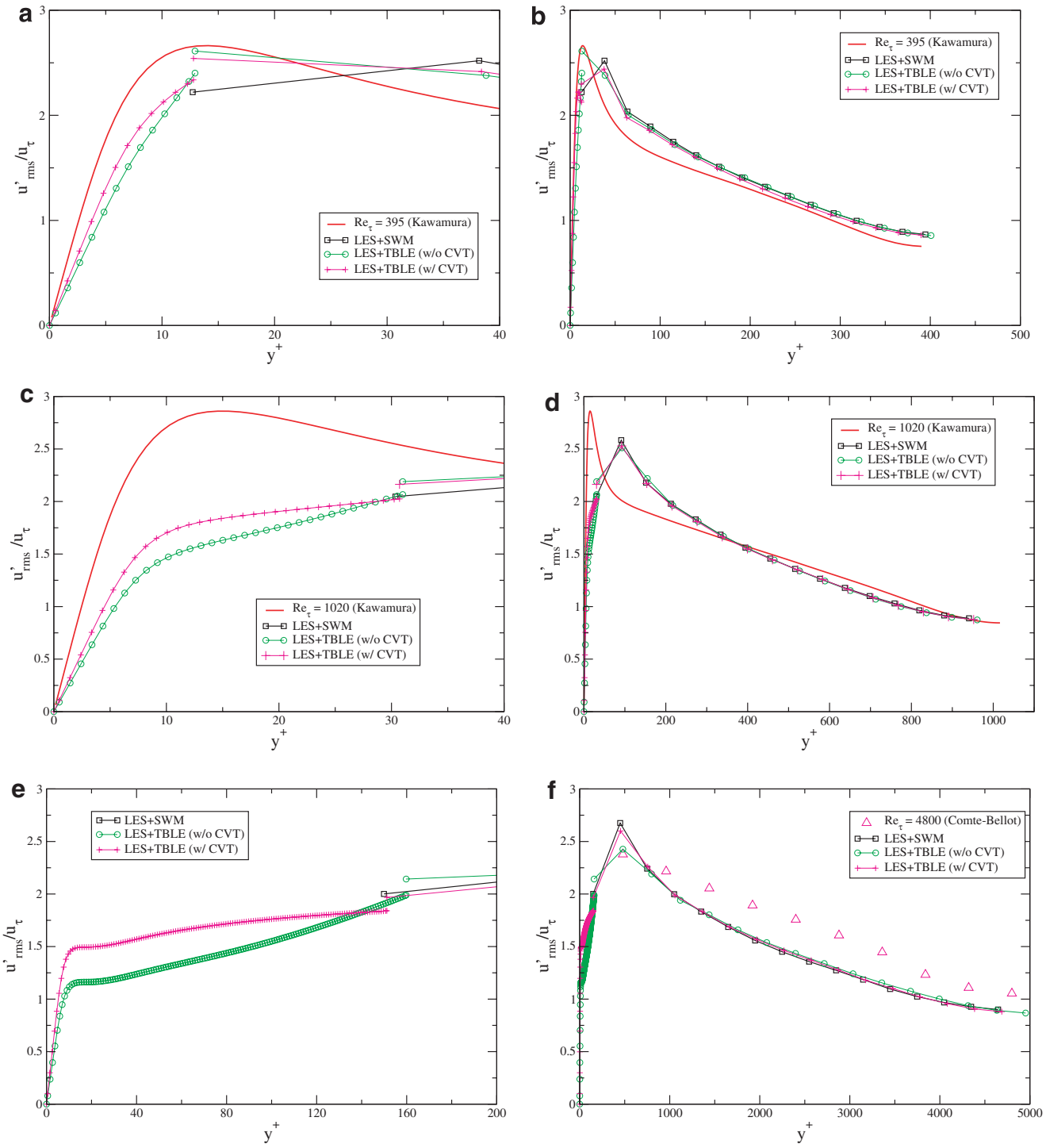

Fig. 4. RMS streamwise velocity fluctuations: (a) TBLE inner mesh, $Re_\tau = 395$, (b) LES outer mesh, $Re_\tau = 395$, (c) TBLE inner mesh, $Re_\tau = 1020$, (d) LES outer mesh, $Re_\tau = 1020$, (e) TBLE inner mesh, $Re_\tau = 4800$ and (f) LES outer mesh, $Re_\tau = 4800$.

numbers ($Re_\tau = 395, 1020, 4800$) have been considered for a single mesh resolution. In the former configuration, the first velocity node of the LES mesh is located in the buffer layer ($y^+ = 12.5$), and in the second configuration it is located in the beginning of the logarithmic region ($y^+ = 32$), see Table 1. The computations performed at $Re_\tau = 395$ and at $Re_\tau = 1020$ are compared to the results of the Abe et al. [1,2] and Kawamura et al. [19]. The computations at $Re_\tau = 4800$ have been carried out to investigate the behavior of the TBLE wall model on a very coarse mesh.

The mesh parameters are displayed in Table 1. A sufficient number of nodes were set in the TBLE mesh so that $\Delta y^+ = 1$ in the TBLE zone.

The standard wall models (SWM) are compared to the TBLE wall models for the velocity and the temperature fields. The results obtained with the various TBLE wall model variants with (noted w/CVT) or without (w/o CVT) convective terms are also compared. The mean profiles of the computations performed at $Re_\tau = 4800$ are compared to analytical laws. To obtain a deeper insight into the TBLE wall behavior, some figures presented in Section 5 are split into two parts: the TBLE fine mesh (inner mesh) and the LES coarse mesh (outer mesh). The statistics are based on plane and time average.

3.1. Velocity field

The mean profiles are shown in Fig. 3 for the velocity field. The mean streamwise velocity field is in perfect agreement with the DNS data for the TBLE velocity field, while, the LES on the coarser mesh exhibits some small discrepancies when the Reynolds number is increased. This is typical of coarse LES results, as already reported by many authors (see [23] and [30]). Besides, for the coarsest mesh (Fig. 3c), the mean velocity profiles in the LES domain obtained with TBLE with convective terms are not better (and even slightly worse) than the profiles obtained without them. However, this behaviour could be due to a cancellation effects of the numerical error induced by the coarseness of the mesh.

Considering fluctuations of velocity or temperature in the TBLE domain could appear as unjustified, given that a RANS model is used to close the equations. However,

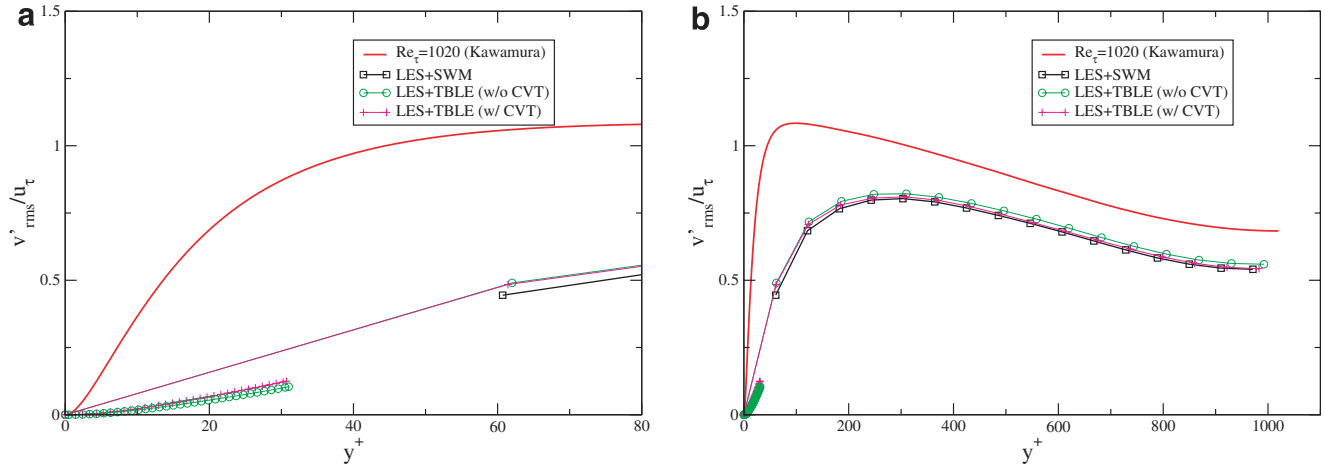

Fig. 5. RMS normal velocity fluctuations profiles: (a) TBLE inner mesh, $Re_\tau = 1020$ and (b) LES outer mesh, $Re_\tau = 1020$.

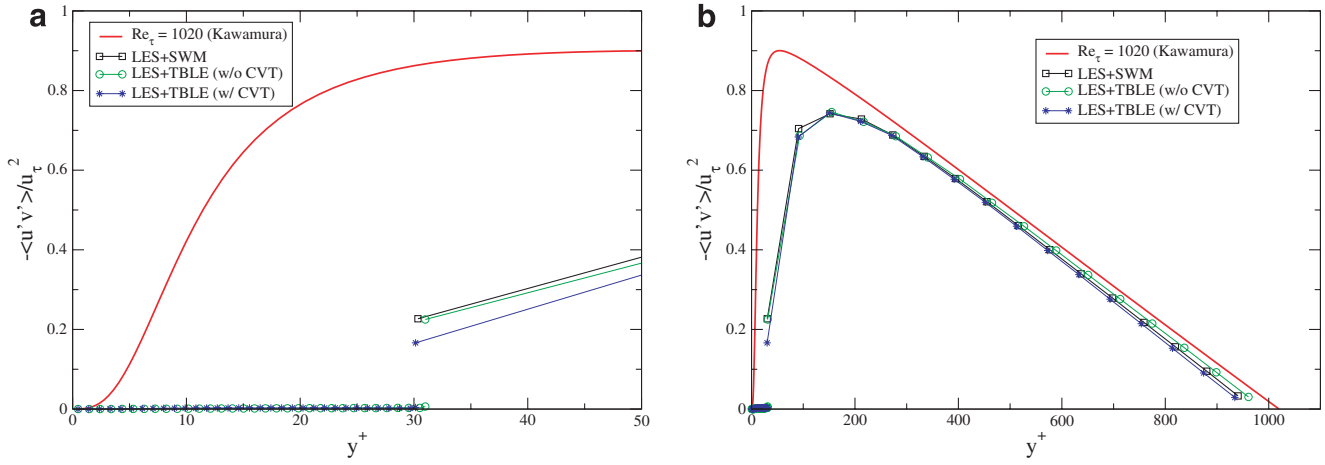

Fig. 6. Reynolds stress profiles: (a) TBLE inner mesh, $Re_\tau = 1020$ and (b) LES outer mesh, $Re_\tau = 1020$.

this point of view can be legitimated relying on the fact that the TBLE inner mesh may convey unsteadiness from the LES mesh to the wall through an unsteady RANS approach.

Observing Fig. 4b, d and f, the RMS velocity fluctuations on the LES mesh exhibit a peak at the second computational node whereas it should be at 15 wall units of the wall (see Sagaut [26]). This feature is a typical drawback of LES in coarse meshes (see Benarafa et al. [6]). Away from the near-wall region, the fluctuations are damped.

Let us focus on Fig. 4a, c and e. First, it can be noticed that RMS velocity fluctuations exist on the TBLE mesh and they are not reduced to a linear link between the outer mesh and the wall. It is to be noted that the TBLE wall model with convective terms mimics the behaviour of the fluctuation peak. Although the level of the fluctuation peak in the TBLE inner mesh is not correct, its location appears to be between 10 and 20 wall units which is in agreement with the physics even on the coarser mesh.

It can be noted that the RMS fluctuations of the streamwise velocity of the inner TBLE mesh and the outer LES mesh do not exactly match at the interface. The velocity at the interface is interpolated at the center of the cell for the TBLE mesh whereas it is not for the LES mesh. Thus, the non-linear statistics (RMS, $\langle u'v' \rangle$, ...) show a discontinuity at the interface whereas the linear statistics (time average, ...) do not.

The temperature field in the TBLE domain does not suffer from the same drawback since the value of the temperature in the LES outer mesh is defined at the center of the cell.

The RMS normal velocity fluctuation profiles (Fig. 5a and b) show that the TBLE profile does not match the LES outer profile. This fact was foreseeable since the TBLE mesh is defined from the wall to the center of the cell whereas the normal velocity of the LES staggered mesh is computed at the wall and at faces at the top of the cell.

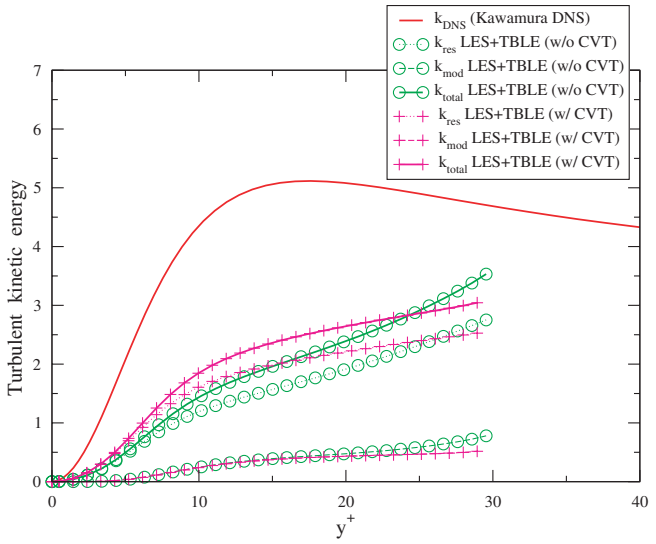

Fig. 7. Turbulent kinetic energy profiles on the TBLE inner mesh at $Re_\tau = 1020$.

Moreover, to compare to the RMS normal velocity fluctuation profile, a straight line between the wall and the normal velocity computational LES node was plotted. Although it is not equal to zero, the RMS normal velocity fluctuation level is quite low compared to the DNS data. The RMS normal velocity fluctuation at the vicinity of the wall seem to be linear in the TBLE inner mesh whereas it should scale as y^{+2} according to Abe et al. [1].

The Reynolds stress (Fig. 6a and b), are very low and almost equal to zero within the inner TBLE mesh and underestimated in the coarse LES mesh.

The poor evaluation of the RMS normal velocity fluctuation and the Reynolds stress is mainly due to two reasons. On the one hand, the TBLE normal velocity is computed thanks to the evaluation of the gradients of u and w (see Eq. (11)) which are both interpolated. This leads us to

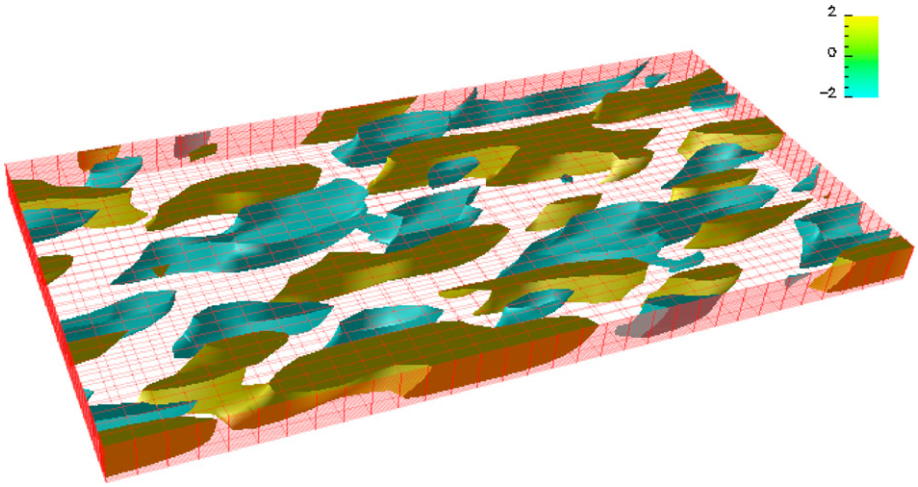

Fig. 8. Isosurfaces of instantaneous streamwise velocity fluctuation ($u' = 0.06U_{\text{bulk}}$ and $u' = -0.06U_{\text{bulk}}$) on the TBLE inner mesh at $Re_\tau = 1020$.

the interpolation problem discussed before. On the other hand, since the LES outer mesh is quite coarse, the numerical estimation of the gradients $\frac{\partial u}{\partial x}$ and $\frac{\partial w}{\partial z}$ might be quite poor.

To further investigate the behavior of the flow in the TBLE inner domain, the resolved turbulent kinetic energy k_{res} and the modeled turbulent kinetic energy k_{mod} were distinguished to build the total turbulent kinetic energy k_{total} which could be the turbulent kinetic obtained with a steady k–ϵ model or computed by a DNS. Thus, the following scale separation was performed:

$$k_{\text{total}} = k_{\text{res}} + k_{\text{mod}} \tag{14}$$

In which k_{res} is computed with the resolved fluctuations of the velocity in the TBLE inner mesh $u_i'^{\text{res}}$:

$$k_{\text{res}} = \frac{1}{2}\langle u_i'^{\text{res}} u_i'^{\text{res}} \rangle \tag{15}$$

k_{mod} is established from the turbulent viscosity computed on the TBLE inner mesh ν_{t} (defined in (12)) considering that the turbulent viscosity is equal to the product of a modeled velocity scale u'^{mod} by a length scale l_{mod}:

$$k_{\text{mod}} = \frac{1}{2}(u'^{\text{mod}})^2 \quad \text{with } u'^{\text{mod}} = \frac{\nu_{\text{t}}}{l_{\text{mod}}} \quad \text{and}$$
$$l_{\text{mod}} = \kappa y D^{1/2} \tag{16}$$

Observing Fig. 7, it is seen that the total kinetic energy in the TBLE inner mesh appears as lower than the DNS data which corroborates the results obtained for RMS streamwise velocity fluctuation. Fig. 7 shows also that the main part of the near-wall turbulent kinetic energy is carried by the resolved component k_{res}, showing that the unsteadiness of the LES mesh plays an essential role. The modeled component of the turbulent kinetic energy k_{mod} is quite low and is very similar for both variants of the TBLE wall model.

The coherent structures in the inner TBLE mesh can be identified thanks to the isosurfaces of the instantaneous streamwise velocity fluctuation (Fig. 8). Since the TBLE inner mesh spreads from the wall to $y^+ = 30$ (for the computation at $Re_\tau = 1020$), the streaky structures shown in Fig. 8 are thicker and flatter than the physical streaks which are well-known features of the turbulent boundary layer. As discussed before, these unphysically large *numerical* streaks have been also observed by Baggett [3]. These streaks are unphysically large because the y cannot be resolved by the grid.

3.2. Temperature field

The temperature mean profiles are shown in Fig. 9. The same kind of analysis as for the velocity field can be performed. Indeed, the mean temperature field in the TBLE domain is in fair agreement with the Kader law at each

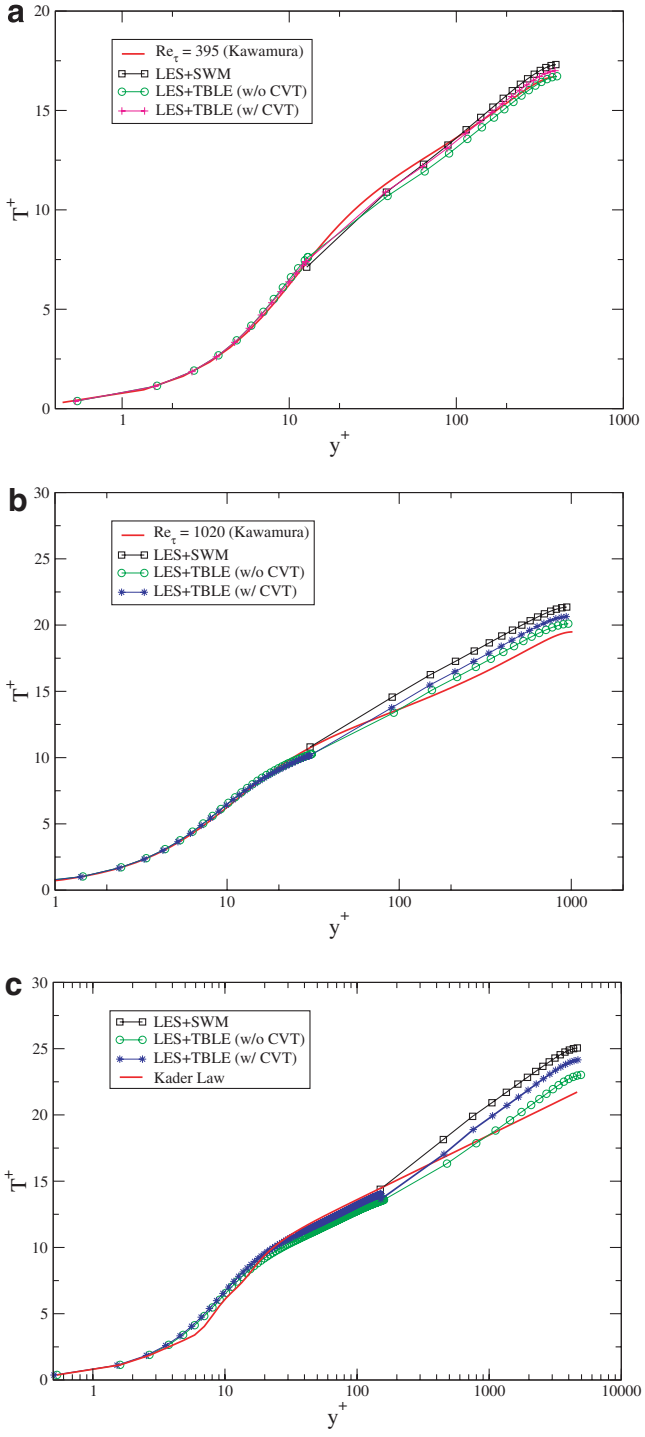

Fig. 9. Mean temperature profiles: (a) $Re_\tau = 395$, (b) $Re_\tau = 1020$ and (c) $Re_\tau = 4800$.

Reynolds number. The sensitivity of the results to grid resolution is similar to what is observed on the velocity field.

The mean profiles are slightly better when the convective terms are removed from the TBLE equation. This could be due to error balance.

The RMS temperature profiles on the LES outer mesh are shown in Fig. 10b, d, and f. Given the coarseness of the mesh, it was foreseeable that the RMS temperature

level will be underestimated. This phenomenon is amplified with the increase of the Reynolds number.

In the TBLE mesh, (Fig. 10a, b and e) the RMS temperature profiles obtained with the TBLE wall model with convective terms are in fair agreement with the DNS data in the viscous sublayer. Moreover, in this region, the slope of the profile is compared to the analytical formula proposed by Teitel et al. [29] to model the behavior of RMS fluctuation of the temperature in the viscous sublayer for an isothermal wall boundary condition:

$$T'^{+}_{\mathrm{rms}} = 0.36 Pry^{+} \tag{17}$$

This empirical law is fully corroborated by the profile of the RMS temperature fluctuations of the TBLE wall

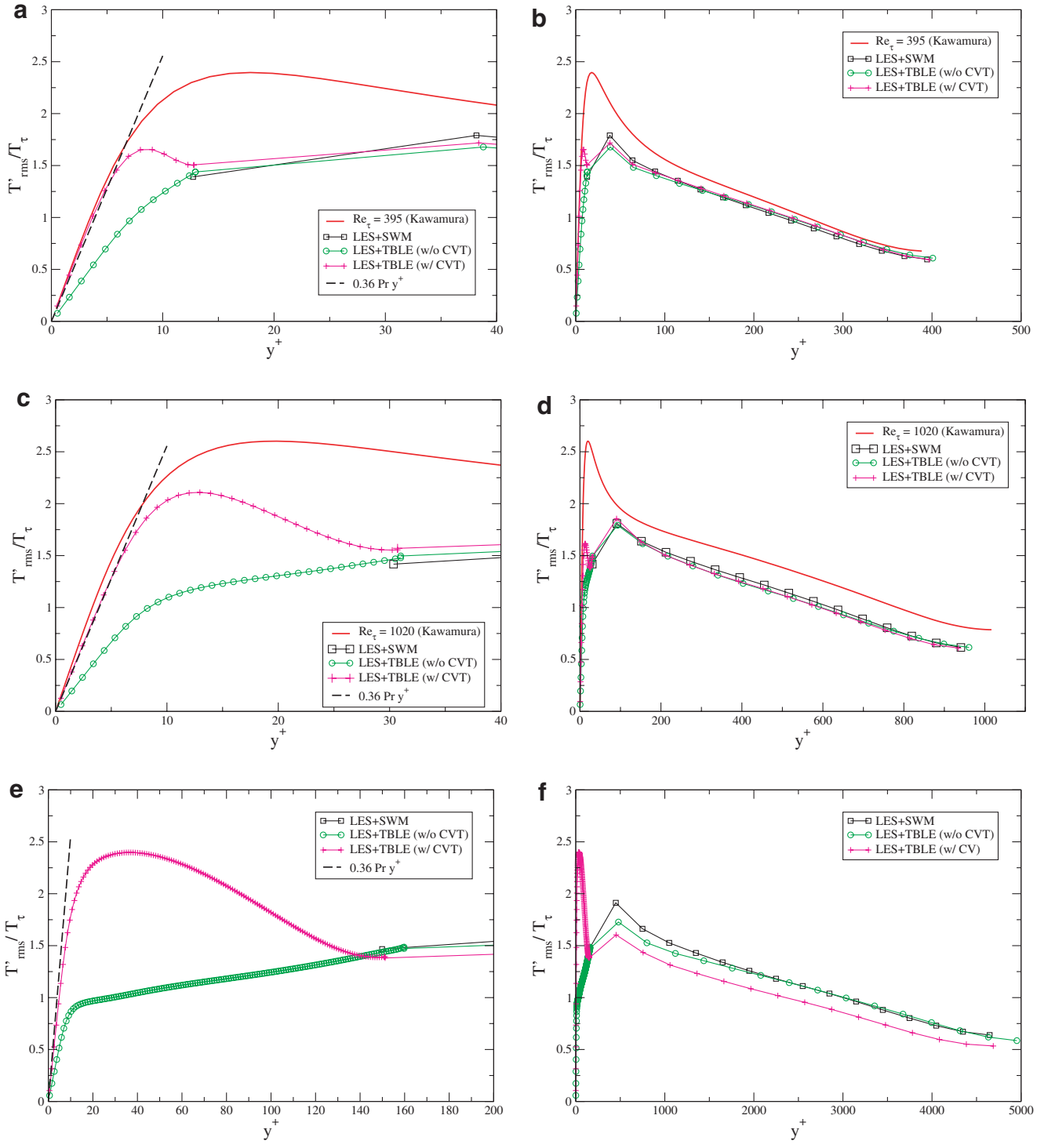

Fig. 10. RMS temperature fluctuations profiles: (a) TBLE inner mesh, $Re_\tau = 395$, (b) LES outer mesh, $Re_\tau = 395$, (c) TBLE inner mesh, $Re_\tau = 1020$, (d) LES outer mesh, $Re_\tau = 1020$, (e) TBLE inner mesh, $Re_\tau = 4800$ and (f) LES outer mesh, $Re_\tau = 4800$.

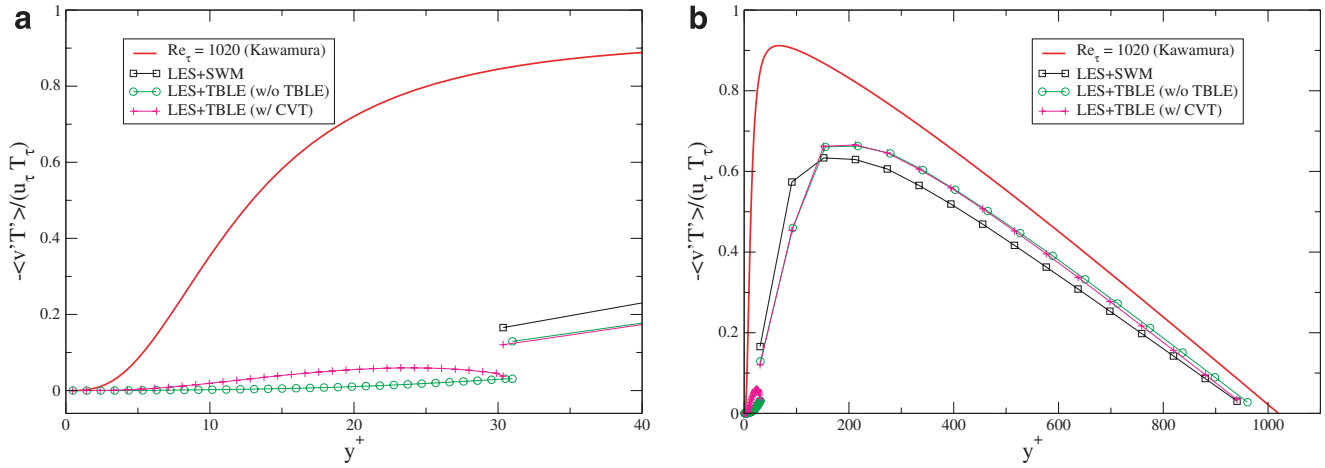

Fig. 11. Resolved normal turbulent heat flux mean profiles: (a) TBLE inner mesh, $Re_\tau = 1020$ and (b) LES outer mesh, $Re_\tau = 1020$.

model with convective terms for each Reynolds number. This result is very encouraging considering the viewpoint of conjugate heat transfer in LES with wall models. Indeed, for high Reynolds number flows in a conjugate heat transfer configuration, the use of wall models becomes necessary and the reconstruction of near-wall fluctuations of the temperature field is a crucial problem as noted by Châtelain et al. [13]. It can also be noticed that the TBLE wall model with convective terms provides a DNS-like behaviour for the RMS temperature fluctuations in the near-wall region, since it creates a peak near to its physical location. However, the level of the peak seems to be slightly underestimated.

One can notice that the RMS temperature profile $\langle T'^2\rangle^{1/2}$ is better captured than the RMS velocity profile $\langle u'^2\rangle^{1/2}$. This may be due to the fact that the temperature is computed at the center of the cell so that the continuity (without interpolation) of the temperature field is ensured at the interface between the TBLE inner layer and the LES outer mesh.

On figures Fig. 11a and b, the resolved normal heat flux are shown. For the TBLE wall model without convective terms, the normal heat flux $\langle v'T'\rangle$ is almost zero, whereas a certain amount of the normal heat flux is captured with the use of the convective terms in the TBLE wall model. This observation can be related to the peak of RMS temperature fluctuations in the TBLE inner mesh shown in Fig. 10a, c and e. Nevertheless, it cannot be denied that the normal heat flux observed in the TBLE inner mesh for TBLE with convective terms remains very low compared to the DNS data. This too low normal heat flux can be explained by the poor evaluation of the normal velocity discussed before. This leads to two comments: (i) it appears that even a poor estimation of the normal velocity and the convection terms in the near-wall may improve significantly the representation of the near-wall behaviour of the temperature fluctuations, (ii) the forcing of the temperature (and consequently of temperature fluctuation) at the top boundary condition of the TBLE inner mesh is responsible for the generation of a large amount of the temperature fluctuation in the TBLE region.

4. Concluding remarks

In this study, the TBLE wall model was analyzed with regard to the near-wall unsteadiness features and a completely new thermal wall model inspired from the former was successfully tested and its results were analyzed.

Although the TBLE wall model yields better results on the overall than standard wall models, it is unable to correct the drawback of the LES outer mesh such as the mean profile mismatch and the spurious location of the fluctuation peak.

The TBLE layer appeared to be able to sustain fluctuations, despite the use of a RANS model. The RMS fluctuations are better represented by the TBLE wall model with convective terms. This observation is particularly true for the RMS temperature fluctuations which reproduce a DNS-like behaviour near the wall. However, these fluctuations (velocity and temperature) are quite low compared to the DNS data. The main reasons are the following. First, the use of a RANS model in the TBLE mesh could contribute to the damping of the fluctuations. Then, the poor evaluation (due to the coarseness of the outer LES mesh) of the normal velocity field in the TBLE mesh induces a spurious evaluation of the convective terms in TBLE. Finally, the upper boundary condition of the TBLE velocity wall model involves (for staggered meshes) an interpolation of the velocity of the LES first node. The last two causes are quite difficult to prevent. The first one could be cured enforcing the continuity the turbulent viscosity at the interface between the TBLE wall model and the LES mesh as suggested by Wang and Moin [31] or Diurno et al. [15]. Nevertheless, it might not be enough to reach a correct RMS fluctuation levels since none of these authors have reported such an improvement. It may only be able to enhance the

RMS fluctuation profile in the inner layer as shown by Temmerman et al. [30].

Moreover, it has to be highlighted that an important result of this study is that, in spite of an unperfect prediction of all the near-wall physics, the thermal TBLE wall model with convective terms is able to recover the wall normal heat flux in fair agreement with the DNS data and corroborating perfectly the Teitel et al. criteria [29]. Although all the physics of the turbulent flow is not captured by the present TBLE model, this result may be promising for conjugate heat transfer problems at high Reynolds number. Indeed, large-eddy simulations applied to this kind of configuration requires wall models which are able to propagate the unsteadiness of the flow from the first LES node to the solid wall. With regard to this requirement, the thermal TBLE wall model has three advantages compared to a classical wall model based on an equilibrium law. First, the upper boundary conditions of the TBLE inner mesh are local in space and instantaneous. Then, the effects of the convectives terms in the TBLE inner mesh can be taken into account. Finally, the equations solved in the TBLE inner mesh are based on an Unsteady RANS method which ensures a better transmission of the unsteadiness of the flow.

References

[1] H. Abe, H. Kawamura, Y. Matsuo, Direct Numerical Simulation of a fully developed turbulent channel flow with respect to the Reynolds Number dependence, J. Fluids Eng. (Trans. ASME) 123 (2001) 383–393.

[2] H. Abe, H. Kawamura, Y. Matsuo, Surface heat-flux fluctuations in a turbulent channel flow up to $Re_\tau = 1020$ with $Pr = 0.025$ and 0.71, Int. J. Heat Fluid Flow 25 (2004) 404–419.

[3] J.S. Baggett, On the feasibility of merging LES with RANS for the near-wall region of attached tubulent flows. Annual Research Briefs – Center for Turbulence Research, 1998, pp. 267–277.

[4] J.S. Baggett, J. Jimenez, A.G. Kravchenko, Resolution requirements in large-eddy simulations of shear flows. Annual Research Briefs – Center of Turbulence Research, 1997.

[5] E. Balaras, C. Benocci, U. Piomelli, Two-layer approximate boundary conditions for large-eddy simulations, AIAA J. 34 (6) (1996) 1111–1119.

[6] Y. Benarafa, O. Cioni, F. Ducros, P. Sagaut, RANS/LES coupling for unsteady turbulent flow simulation at high Reynolds number on coarse meshes, Computer Meth. Appl. Mech. Eng. 195 (23–24) (2006) 2939–2960.

[7] W. Cabot, Large-eddy simulations with wall-models. Annual Research Briefs – Center for Turbulence Research, 1995, pp. 41–50.

[8] W. Cabot, Near-wall models in large eddy simulations of flow behind a backward facing step. Annual Research Briefs – Center for Turbulence Research, 1996, pp. 199–210.

[9] W. Cabot, P. Moin, Approximate wall boundary conditions in the large-eddy simulation of high reynolds number flow, Turbul. Combust. 63 (2000) 269–291.

[10] C. Calvin, O. Cueto, P. Emonot, An object-oriented approach to the design of fluid mechanics software, Math. Model. Numer. Anal. 36 (5) (2002) 907–921.

[11] D.R. Chapman, Computational aerodynamics development and outlook, AIAA J. 17 (12) (1979) 1293–1313.

[12] A. Châtelain, F. Ducros, O. Metais, LES of heat transfer: proper numerical schemes for temperature transport, Int. J. Numer. Meth. Fluids 44 (2004) 1017–1044.

[13] A. Châtelain, F. Ducros, O. Metais, Large Eddy Simulation of conjugate heat-transfer using thermal wall functions, in: R. Friedrich et al. (Eds.), Direct and large-eddy simulation V, Kluwer Academic Publishers, 2004, pp. 307–314.

[14] R.B. Dean, Reynolds number dependence of skin friction and other bulk flow variables in two-dimensional rectangular duct flow, J. Fluids Eng. 100 (1978) 215–223.

[15] G.V. Diurno, E. Balaras, U. Piomelli, in: B. Geurts (Ed.), Wall-layer models for LES of separated flows, RT Edwards, Philadelphia, PA, 2001, pp. 207–222, chapter 11.

[16] P. Emonot, Méthodes de Volumes Elements Finis: Application aux equations de Navier–Stokes et résultats de convergence. PhD thesis, Université Claude Bernard – Lyon I, 1992 (In French).

[17] G. Grötzbach, Direct and large eddy simulation of turbulent channels flows, in: N.P. Cheremisinoff (Ed.), Encyclopedia Fluids Mech., Gulf Publ., West Orange, NJ, 1987, pp. 1337–1391.

[18] C.V. Hirt, B.D. Nichols, N.C. Romero, Sola – a numerical solution algorithm for transient flow. Technical report, Los Alamos National Laboratory, Report LA-5852, 1975.

[19] H. Kawamura, K. Ohsaka, H. Abe, K. Yamamoto, DNS of turbulent heat transfer in channel flow with low to medium-high Prandtl number fluid, Int. J. Heat Fluid Flow 19 (1998) 482–491.

[20] A. Kerstein, One-dimensional turbulence: model formulation and application to homogeneous turbulence, shear flows, and buoyant stratified flows, J. Fluid Mech. 392 (1999) 277–334.

[21] J. Kim, P. Moin, R. Moser, Turbulence statistics in fully developed channel flow at low reynolds number, J. Fluid Mech. 177 (1987) 133–166.

[22] M. Lesieur, O. Metais, New trends in large-eddy simulations of turbulence, Ann. Rev. Fluid. Mech. 28 (1996) 45–82.

[23] F. Nicoud, J.S. Baggett, P. Moin, W. Cabot, Large eddy simulation wall-modelling based on suboptimal control theory and linear stochastic estimation, Phys. Fluids 13 (10) (2001) 2968–2984.

[24] N.V. Nikitin, F. Nicoud, B. Wasistho, K.D. Squires, P.R. Spalart, An approach to wall modeling in large-eddy simulations, Phys. Fluids 12 (7) (2000) 1629–1632.

[25] U. Piomelli, E. Balaras, Wall-layer models for large-eddy simulations, Ann. Rev Fluid Mech. 34 (2002) 349–374.

[26] P. Sagaut, Large Eddy Simulation for Incompressible Flows, third ed., Springer Verlag, 2005.

[27] R.C. Schmidt, A.R. Kerstein, S. Wunsh, V. Nilsen, Near-wall les closure based on one-dimensional, J. Comput. Phys. 186 (2003) 317–355.

[28] P.R. Spalart, Strategies for turbulence modelling and simulations, Int. J. Heat Fluid Flow 21 (2000) 252–263.

[29] M. Teitel, R. Antonia, Heat transfer in fully developed turbulent channel flow: comparison between experiment and direct numerical simulations, Int. J. Heat Mass Transfer 36 (6) (1993) 1701–1706.

[30] L. Temmerman, M. Hadziabdic, M.A. Leschziner, K. Hanjalic, A hybrid two-layer URANS-LES approach for large-eddy simulation at High Reynolds numbers, Int. J. Heat Fluid Flow 26 (2005) 173–190.

[31] M. Wang, P. Moin, Dynamic wall modeling for large-eddy simulation of complex turbulent flows, Phys. Fluids 14 (7) (2002) 2043–2051.